

The Role of Helium Stars in the Formation of Double Neutron Stars

N. Ivanova¹, K. Belczynski^{1,2}, V. Kalogera¹, F.A. Rasio¹, & R.E. Taam¹

¹ *Northwestern University, Dept. of Physics & Astronomy, 2145 Sheridan Rd., Evanston, IL 60208*

² *Lindheimer Postdoctoral Fellow*

nata, belczynski, vicky, rasio, r-taam@northwestern.edu

ABSTRACT

We have calculated the evolution of 60 model binary systems consisting of helium stars in the mass range of $M_{\text{He}} = 2.5 - 6 M_{\odot}$ with a $1.4 M_{\odot}$ neutron star companion to investigate the formation of double neutron star systems. Orbital periods ranging from 0.09 to 2 days are considered, corresponding to Roche lobe overflow starting from the helium main sequence to after the ignition of carbon burning in the core. We have also examined the evolution into a common envelope phase via secular instability, delayed dynamical instability, and the consequence of matter filling the neutron star's Roche lobe. The survival of some close He-star neutron-star binaries through the last mass transfer episode (either dynamically stable or unstable mass transfer phase) leads to the formation of extremely short-period double neutron star systems (with $P \lesssim 0.1$ days). In addition, we find that systems throughout the entire calculated mass range can evolve into a common envelope phase, depending on the orbital period at the onset of mass transfer. The critical orbital period below which common envelope evolution occurs generally increases with M_{He} . In addition, a common envelope phase may occur during a short time for systems characterized by orbital periods of 0.1 - 0.5 days at low He-star masses ($\sim 2.6 - 3.3 M_{\odot}$).

The existence of a short-period population of double neutron stars increases the predicted detection rate of inspiral events by ground-based gravitational-wave detectors and impacts their merger location in host galaxies and their possible role as γ -ray burst progenitors. We use a set of population synthesis calculations and investigate the implications of the mass-transfer results for the orbital properties of DNS populations.

Subject headings: binaries: close — stars: evolution — stars: neutron — stars: formation

1. INTRODUCTION

The formation of double neutron star (DNS) systems is thought to be the endpoint of long sequences of evolutionary stages involving massive binaries (e.g., Bhattacharya & van den Heuvel 1991, Belczynski et al. 2002b). Although a complete understanding of the detailed DNS formation channels remains to be attained, the observational characteristics of observed DNS systems clearly indicate the involvement of massive stars and mass-transfer phases that can lead to dramatic orbital contraction (e.g., common-envelope phases) prior to the formation of the second-born neutron stars. Uncovering the details of DNS formation and its dependence on the outcomes of prior binary evolution phases has important implications for our understanding of binary-pulsar formation (van den Heuvel & Taam 1984), supernovae of hydrogen-poor stars (Nomoto et al. 1994), sources of gravitational waves (Clark & Eardley 1977), and possibly γ -ray bursts (Paczynski 1986).

One of the intermediate evolutionary stages of DNS formation involves binaries with first-born neutron stars (NS) and helium-rich companions. This stage follows that of the high-mass X-ray binaries (NS with massive, hydrogen-rich companions). In this study we focus on the role of such helium-rich NS companions in DNS formation mechanisms. In particular we investigate the response of helium stars to binary mass transfer driven by Roche lobe overflow. Our calculations are in some ways complementary to those presented by Dewi et al. (2002), and we address the issue of the outcome of mass transfer episodes in the context of DNS formation. We are especially interested in (i) the degree of orbital contraction (if any) during mass transfer driven by the helium star, (ii) the possible development of mass transfer on dynamical time scales and of a common-envelope (CE) phase (Taam & Sandquist 2000), and (iii) the possible merger of the binary, aborting DNS formation.

The outcome of this last episode of mass transfer in DNS progenitors has important implications for the distribution of orbital separations and, hence, of gravitational-wave merger lifetimes of DNS systems and the location of merger sites relative to host galaxies. In this context, Belczynski et al. (2002b) have explored the implications of the *assumption* that *low-mass* helium giants ($M \lesssim 4.5M_{\odot}$) (Habets 1986; Woosley et al. 1995) develop sufficiently deep convective envelopes to drive mass transfer onto NS on dynamical time scales and therefore evolve into a CE phase. Under this assumption they found that a large fraction of binaries can survive this phase. Subsequent evolution leads to the explosion of the helium star core in a Type Ic supernova and the formation of very tight DNS systems with merger lifetimes shorter than a few Myr. Systems with such short lifetimes would be difficult to detect as binary radio pulsars relative to the known systems with longer lifetimes (Belczynski et al. 2002b) and would not have sufficient time to escape their host galaxies (Belczynski et al. 2002a; Belczynski et al. 2002c; Perna & Belczynski 2002) before

merging. We point out that Belczynski et al. (2002b) had also taken into account the effects of hyper-critical accretion onto the NS during the CE phases (Brown 1995). Despite some accretion, both during the H-rich CE phase (end of X-ray binary stage) and the He-rich CE phase (last binary interaction) in DNS formation scenarios, the NS avoids collapse into a black hole. These results are based on calculations of the mass accretion rate onto NS and the assumption that the maximum NS mass is greater than $\simeq 1.5M_{\odot}$ [for more details see Belczynski et al. (2002a)].

In this study we perform detailed binary evolutionary calculations relevant to helium stars overflowing their Roche lobes and transferring matter to their NS companions. The calculations cover a range of helium-star masses ($M_{\text{He}} = 2.5 - 6 M_{\odot}$) and evolutionary stages that are relevant to DNS formation. For each sequence, the temporal evolution of the mass-transfer rate and orbital period are calculated and the outcome of the mass transfer (dynamical or thermal instability or merger) is examined. Since thermal instability can lead to high mass transfer rates, in excess of the NS Eddington limit, we examine its consequences in the context of considerations of the *trapping radius* [i.e., the characteristic radius for mass loss due to super-Eddington mass transfer (Begelman 1979)] and the possibility that a common-envelope phase develops (King & Begelman 1999). The results delineate the parameter regime (mass of the helium star and the orbital period at the onset of mass transfer) where systems survive as binaries from those where the systems merge. Using the *StarTrack* population synthesis code (Belczynski et al. 2002b) we examine the implications of these results for the physical characteristics of DNS populations and present our results.

In the following section we describe our computational methods and initial models both for the mass transfer sequences and the DNS population synthesis calculations. In section §3 we describe our results in detail and in section §4 we discuss their implications for DNS formation, binary models for hydrogen-poor supernovae, gravitational waves, and γ -ray bursts.

2. METHODS AND INITIAL MODELS

2.1. Mass-Transfer Sequences

For the mass transfer calculations we have used a standard Henyey-type stellar evolution code (Kippenhahn et al. 1967), recently updated by Podsiadlowski et al. (2002). We have adopted OPAL opacities (Rogers & Iglesias 1992), supplemented with contributions from atomic, molecular and grain absorption in the low temperature regime ($\lesssim 12,500$ K) (Alexander & Ferguson 1994). The nuclear reactions (tracking 40 isotopes) describe the

major burning stages through oxygen burning with rates taken from Thielemann’s library REACLIB (Thielemann et al. 1986) and updated as in Cannon (1993)¹.

We have calculated models for zero-age Main-Sequence helium stars (HeMS) with a solar metallicity ($Y = 0.98, Z = 0.02$). Since such stars are characterized by convective cores and can evolve to include convective envelopes, we have adopted the Schwarzschild convection criterion with a mixing-length parameter $\alpha = 2$ and a convective-overshooting parameter equal to 12% of the pressure scale height H_P . We have also included in the models mass loss associated with stellar winds with rates given by Hurley et al. (2000) as

$$\dot{M}_{\text{He,wind}} = - \max \left[2 \times 10^{-13} \frac{LR}{M}, 10^{-13} L^{1.5} \right] M_{\odot} \text{ yr}^{-1} . \quad (1)$$

Here, M , R , and L are the stellar mass, radius and luminosity in solar units.

To determine the adequacy of our stellar models, we have carried out evolutionary sequences to the stage of oxygen core burning for single helium stars with masses in the range of 2 to 6 M_{\odot} . We have found the internal structure as well as the radii of our models at various evolutionary stages to be in good agreement with results obtained by Habets (1986), Dewi et al. (2002), Pols (2002), and Woosley (1997).

We have calculated binary mass-transfer sequences assuming a NS mass $M_{\text{NS}} = 1.4M_{\odot}$ and initial helium star masses $M_{\text{He},0}$ in the range 2.5–6 M_{\odot} . We have chosen the orbital period P_{tr} at the onset of the mass transfer as the main input parameter for our mass transfer sequences. For a given value of P_{tr} and $M_{\text{He},0}$ we calculated the age at which this star will overflow its Roche lobe by evolving the helium star from the ZAMS to the onset of mass transfer as a single star. We typically start the binary sequences at an evolutionary age slightly before Roche lobe overflow and followed the evolution until core-oxygen burning, unless we encounter conditions leading to a binary merger.

During Roche lobe overflow, mass transfer rates are calculated following the prescription adopted in Tout & Eggleton (1988)

$$\dot{M}_{\text{tr}} = 10^3 \times \max [0, (\ln(R/R_{\text{RL}}))^3] M_{\odot} \text{ yr}^{-1}, \quad (2)$$

where R_{RL} is the Roche-lobe radius and is given as a function of the binary mass ratio

¹The reaction rates have been compared to the recent compiled NACRE reaction rates (Angulo et al 1999). Differences of less than 5% are found for important reaction rates in the required temperature range. Since the triple- α reaction rates are highly temperature sensitive the differences are inconsequential for the evolution.

$q \equiv M_{\text{He}}/M_{\text{NS}}$ and the orbital separation A by (Eggleton 1983)

$$R_{\text{RL}} = \frac{0.49q^{2/3}}{0.6q^{2/3} + \ln(1 + q^{1/3})} A . \quad (3)$$

During detached phases we also account for the effects of mass transfer due to *atmospheric* Roche lobe overflow. We use a prescription by Ritter (1988) for the mass transfer rate calculation

$$\dot{M}_{\text{tr}} = \dot{M}_0 \exp\left(\frac{R_{\text{RL}} - R}{H_P}\right) , \quad (4)$$

where \dot{M}_0 is the mass transfer rate when the mass losing star fills its Roche lobe, $\dot{M}_0 = \frac{1}{\sqrt{e}} \rho_{\text{ph}} v_s Q$. Here ρ_{ph} is the photospheric density of the helium star, v_s is the isothermal sound speed and $Q \approx R_{\text{RL}} H_P$ is the effective cross section of the gas stream at the inner Lagrangian point, L_1 . The total rate at which the helium star loses mass is

$$\dot{M}_{\text{He}} = -\dot{M}_{\text{tr}} + \dot{M}_{\text{He,wind}} . \quad (5)$$

Throughout our mass-transfer sequences we have assumed that NS can accrete only through the mass transfer process, i.e., there is no wind accretion and the mass accretion rate is Eddington limited:

$$\dot{M}_{\text{accr}} = \min\{\dot{M}_{\text{tr}}, \dot{M}_{\text{edd}}\} , \quad (6)$$

where

$$\dot{M}_{\text{edd}} \equiv \frac{4\pi c R_{\text{NS}}}{\kappa} . \quad (7)$$

Here c is the speed of light, R_{NS} is the radius of the NS (assumed to be 10 km) and κ is the electron scattering opacity of helium rich material. The orbital evolution is calculated assuming that, if the mass transfer rate exceeds the NS Eddington limit, the excess material escapes the system isotropically with the NS specific orbital angular momentum. This mass loss combined with the isotropic wind mass loss leads to loss of binary orbital angular momentum at a rate given by (van den Heuvel 1994; Kalogera & Webbink 1996; Soberman et al. 1997)

$$\frac{\dot{J}_{\text{ML}}}{J_{\text{orb}}} = \frac{\gamma + \beta q^2}{1 + q} \frac{\dot{M}_{\text{He}}}{M_{\text{He}}} , \quad (8)$$

where $\gamma \equiv \dot{M}_{\text{He,wind}}/\dot{M}_{\text{He}}$ and $\beta \equiv -(\dot{M}_{\text{tr}} - \dot{M}_{\text{accr}})/\dot{M}_{\text{He}}$.

We have also included angular momentum losses due to gravitational radiation at a rate (Landau & Lifshitz, 1958)

$$\frac{\dot{J}_{\text{gw}}}{J_{\text{orb}}} = -\frac{32G^3}{5c^5} \frac{M_{\text{He}} M_{\text{NS}} (M_{\text{He}} + M_{\text{NS}})}{A^4} . \quad (9)$$

We have examined 60 models for helium stars with masses in the range $2.5\text{--}6 M_{\odot}$ for a wide range of orbital separations. Although we mainly focus on sequences where mass transfer is initiated after the end of core-helium burning, we also include a few calculations for systems that reached Roche lobe overflow (RLOF) during the core helium burning phase. The initial parameters for the representative mass-transfer sequences are given in Table 1.

2.2. Population Synthesis Models

To examine the effects of the calculated mass-transfer sequences on the physical properties of DNS populations, we have incorporated our results into a recently developed population synthesis code *StarTrack*. A detailed description of this code can be found in Belczynski et al. (2002b). With *StarTrack* we can follow the evolution of a large ensemble of single and binary stars through long evolutionary sequences, for a large range of masses and metallicities. The single star evolution is based on the analytic fits provided by Hurley et al. (2000) with some modifications related to the determination of compact object masses. The modeling of binary evolution incorporates detailed treatment of stable and unstable, conservative and non-conservative mass transfer episodes, mass and angular momentum loss through stellar winds (dependent on metallicity) and gravitational radiation, hyper-accretion onto compact objects, and asymmetric core collapse events with a realistic spectrum of compact object masses. It further includes an orbit calculator that allows us to model the motion of all systems in gravitational potentials of galaxies (Belczynski et al. 2002c).

Common-envelope evolution is calculated based on the commonly used energy-balance formulation (Tutukov & Yungelson 1979), where orbital energy is consumed with a certain efficiency α_{CE} to balance the envelope binding energy $\alpha_{\text{CE}}\Delta E_{\text{orb}} = E_{\text{bind}}$. The latter energy is proportional to the inverse of a numerical factor λ that describes the degree of central concentration of the mass donor $E_{\text{bind}} \propto 1/\lambda$ (de Kool 1990; Dewi & Tauris 2000). The product $\alpha_{\text{CE}}\lambda$ is typically treated as a free parameter in the models, and in the present study we explore 3 models: 1, 0.3 and 3. We note that although α_{CE} and λ are physically separate parameters, varying them independently is mathematically equivalent to varying their product. The NS masses are obtained from a mapping between the final CO core mass of a given pre-SN star (Hurley et al. 2000) and the final Fe-Ni core mass for a given CO core mass based on models of Woosley (1986). Since hydrodynamical calculations (Fryer 1999) show that there is little fall back during NS formation, we assume that the Fe-Ni core collapses and forms a NS, with a mass equal to the baryonic mass of the collapsing core. The rest of the pre-SN star is lost in the explosion. Asymmetric supernova events are modeled with NS natal kicks of random direction and magnitudes drawn from the Cordes & Chernoff

(1998) distribution (a weighted sum of two Maxwellians, one with $\sigma = 175 \text{ km s}^{-1}$ (80%) and the second with $\sigma = 700 \text{ km s}^{-1}$ (20%). In this study all other model parameters are assumed as in Model A in Belczynski et al. (2002b).

As noted in the Introduction, the version of StarTrack used in Belczynski et al. 2002b adopted the following set of assumptions regarding the behavior of Roche-lobe filling helium stars: (i) helium stars that reach Roche overflow during HeMS were assumed to lead to mergers; (ii) low-mass ($\leq 4 M_{\odot}$) helium stars that have evolved beyond the HeMS were assumed to have developed sufficiently massive convective envelopes to drive mass transfer on dynamical time scales leading the binary to a CE phase. Evolution through the CE phase was treated as described above. In the present study we compare the properties of DNS populations formed under these assumptions and under two other sets of assumptions that are developed based on our detailed mass transfer calculations presented here. These two new sets of assumptions are described in §3.2.

3. NUMERICAL RESULTS

3.1. Mass-Transfer Sequences

Examination of the 60 model sequences reveals that He-star NS binaries can experience stable or unstable mass transfer episodes. Systems which enter the mass-transfer phase during or after He-shell burning are found to exhibit the same qualitative behavior. For example, the evolution of a binary with a $4 M_{\odot}$ He-star filling its Roche lobe during the He-shell burning stage (initial orbital period equal to 0.1 d) is illustrated in Figure 1. It can be seen that the binary experiences two episodes of mass transfer, first during He-shell burning and the second after core-C ignition. This result is typical for all such close binary systems in which the mass transfer is initiated during He-shell burning and is in agreement with the results obtained by Dewi et al. (2002). Between these two mass transfer episodes the system is detached for a few thousand years. During this detached stage the helium star is entirely radiative; the entropy in the very outer layers of the helium star envelope increases. In particular, for periods $P_{\text{tr}} \geq 0.2 \text{ d}$ ($M_{\text{He};0} \leq 3.5 M_{\odot}$) and $P_{\text{tr}} \geq 0.3 \text{ d}$ ($M_{\text{He};0} > 3.5 M_{\odot}$), the entropy in the outer radiative layer increases sufficiently that the mass transfer rate during the second mass transfer event is generally higher than during the first stage. On the other hand, for a binary that entered Roche lobe overflow shortly before the core-C ignition stage, mass transfer is uninterrupted (e.g., for binaries with orbital period at the onset of mass transfer of $P_{\text{tr}} \simeq 0.3 \text{ d}$). Similarly, binaries with more evolved helium stars (past He-shell burning) and wider orbital separations experience only one mass transfer episode after core-C ignition.

The binary separation decreases throughout the evolution as a result of the mass ejection from the system. For the example illustrated in Figure 1, the orbital period decreased by about a factor of 2. In general, for the majority of sequences, the orbital period is decreased by factors as large as 4. We note that, for the system presented in Figure 1, the mass transfer rate exceeds the NS Eddington accretion rate during the entire Roche-lobe overflow phase, and the bulk of the He-rich material is ejected from the binary with the specific orbital angular momentum of the NS.

For those systems in which mass transfer becomes unstable, the systems may enter a CE phase. It is well known that there are two circumstances under which a binary system can undergo CE evolution (Taam & Sandquist 2000): either due to a secular instability or due to a mass transfer episode on a dynamical timescale.

For the secular instability to develop, the moment of inertia of the non-compact and larger star must exceed one third of the orbital moment of inertia of the binary system (e.g., Hut 1980, for a review see Rasio 1996). If the moment of the inertia of the helium star is written as $I_{\text{He}} = k^2 M_{\text{He}} R_{\text{He}}^2$, where k is the dimensionless gyration radius of the He-star, the condition for the development of the instability is

$$k^2 > \frac{1}{3f^2 r_{\text{RL}}^2} \frac{1}{1+q}, \quad (10)$$

where $f \equiv R_{\text{He}}/R_{\text{RL}} \leq 1$, and $r_{\text{RL}} = R_{\text{RL}}/A$. This condition leads to $k^2 > 0.25/f^2$ for $M_{\text{He};0} = 6M_{\odot}$ and $k^2 > 0.65/f^2$ for $M_{\text{He};0} = 2.5M_{\odot}$. Note that $k^2 = 0.4$ for a uniform solid sphere. Since the value of k decreases with more evolved phases and $k^2 = 0.08$ for a zero age HeMS, this condition can never be satisfied for He stars, and the systems with He-star and NS components are secularly stable.

In contrast, mass transfer can be driven on a dynamical timescale, if the helium star develops a sufficiently deep and massive convective envelope. In this case, the envelope tends to expand on a dynamical timescale upon mass loss (Webbink 1985). It was shown by Habets (1986) that only helium stars less massive than $2.5 M_{\odot}$ would develop deep and massive convective envelopes. More massive evolved helium stars can also develop substantial convective envelopes characterized by a large *radial* extent in the late evolutionary stages. However, for these stars only a very small mass fraction may be contained in the outer convective zone. We find that single helium stars of mass greater than $3 M_{\odot}$, evolved with wind mass loss, do not develop a sufficiently massive outer convective zone to initiate a CE phase since the mass contained in this zone is smaller than $0.01\% M_{\text{He}}$. To illustrate this point, we show in Figure 2 (top panels) the internal structure of a $4 M_{\odot}$ He-star just after it has evolved off the MS and after it has begun core-C burning. The convective zones are shown as hatched regions on the entropy plots. For this model we found convection

only in the center of the He-star. Had we evolved a $4 M_{\odot}$ model without mass loss (not realistic, as He-stars are known to have significant wind mass loss) we would have found a small outer convection zone ($\lesssim 0.03 M_{\odot}$). In both cases (either no or very little mass in the outer convection zone) the He-star behaves as a radiative star contracting upon mass loss (Webbink 1985). We note that, although the evolved helium stars (after core He burning) more massive than $\sim 3 M_{\odot}$ transfer mass at highly super-Eddington rates (the Eddington limit for helium accretion $\dot{M}_{\text{NS,edd}} \approx 3 \times 10^{-8} M_{\odot} \text{yr}^{-1}$), the rates are not high enough to drive dynamically unstable mass transfer and initiate a CE phase (e.g., see Figure 1). Only for He-stars less massive than $2.5 M_{\odot}$ and for most evolved He-stars (after core-C ignition) in binaries with orbital periods at the onset of mass transfer in excess of ~ 1 year does a substantial convective envelope develop, leading to a dynamical mass transfer instability and CE evolution.

For donor stars with mostly radiative envelopes, it has been pointed out that a *delayed* dynamical instability can develop (Webbink 1985; Hjellming 1989). This occurs during the thermally unstable mass transfer phase (where the mass ratio of donor to accretor is greater than 1.4) when the steep surface entropy profile has been removed. For a donor star that has not had sufficient time to relax to thermal equilibrium, deeper layers with flat entropy profile can be exposed. Subsequent mass loss then leads then to stellar expansion. Typical critical mass ratios above which the delayed dynamical instability occurs lie between 2, at the beginning of the hydrogen main sequence, and 4, near the base of hydrogen giant branch (Hjellming 1989). In the present calculations we find that the development of the delayed dynamical instability is unavoidable in binaries in which mass transfer is initiated on or soon after the HeMS for the entire studied He-star mass range and for all He-stars (independent of their evolutionary stage at the onset of mass transfer) in binaries with mass ratios exceeding 4. The question then arises as to whether these binaries can survive the ensuing CE phase. Our calculations suggest that they are not likely to survive. In the lower panels of Figure 2 we show the orbital energy as well as the minimum energy E_{min} needed to unbind envelope material for two evolutionary stages. The quantity E_{min} is determined from an integration over the mass contained above the core to the stellar surface as

$$E_{\text{min}} = \int_{M_{\text{core}}}^{M_{\text{He}}} \left(-\frac{GM_r}{r} + H(r) \right) dm , \quad (11)$$

where $H(r)$ is the *specific enthalpy*, M_{core} is the mass of the core of helium star, and M_r is the mass inside a given radius r . The internal energy that is included in the enthalpy corresponds to that of a fully ionized gas decreased by the ionization energy in partially ionized layers of the envelope. We assume that the recombination energy does not play a role in driving the helium envelope expansion. The change in the orbital energy during the

spiral-in process is given by

$$\Delta E_{\text{orb}} = \frac{GM_{\text{core}}M_{\text{NS}}}{2A_f} - \frac{GM_{\text{HE}}M_{\text{NS}}}{2A}, \quad (12)$$

where A_f is the final (after the CE-phase) orbital separation. Soon after the HeMS the orbital energy is smaller than the envelope binding energy except very deep in the He-star interior (see Figure 2). Examination of models at masses other than $4M_{\odot}$ show the same quantitative behavior. Therefore, we conclude that the outcome of the mass transfer and following CE phase in such close binaries is a merger. If mass transfer and the delayed dynamical instability develop during or after core-C burning, the binary might avoid a merger, but only if the transfer of energy from the orbit to the envelope is efficient ($\gtrsim 50\%$; see Figure 2). If only about half or less energy will be converted to the energy driving the expansion of the envelope, the final binary separation will have been reduced to such an extent that the core of the helium star overfills its own Roche lobe and a merger will take place. However, if a significant fraction of the envelope ($> 50\%$) is removed prior to the common envelope phase, then the binary could survive the CE.

In addition to the above two channels for CE evolution, systems involving mass transfer onto a NS may also develop a CE provided that the trapping radius exceeds the Roche lobe radius of the NS (King & Begelman 1999). The trapping radius is the radius at which the luminosity generated by infall of the material reaches the Eddington limit. It is calculated by setting the infall speed of the gas equal to the approximate outward photon diffusion speed of the radiation (for details see King & Begelman 1999). Interior to this radius photon diffusion outwards cannot overcome the advection of matter moving inwards. If the accreting compact object is a black hole, the radiation that is generated in excess of the Eddington limit can be swept into the black hole and lost. However, if the compact object is a neutron star, radiation pressure resists inflow at a rate in excess of the Eddington limit, causing the stellar envelope to grow outwards.

Here the trapping radius, where expulsion of some of the material transferred from a star takes place, is given by (Begelman 1979)

$$R_{\text{trap}} = \frac{\dot{M}}{\dot{M}_{\text{NS,edd}}} \frac{R_{\text{NS}}}{2}, \quad (13)$$

where \dot{M} is the accretion rate. For the case when the accreted matter is helium rich one finds

$$R_{\text{trap}} = 6.4 \times 10^{13} [\text{cm}] \dot{m}, \quad (14)$$

where \dot{m} is the accretion rate in $M_{\odot} \text{ yr}^{-1}$. This criterion can be reexpressed in terms of a critical mass transfer rate. If the mass transfer rate driven by the donor is higher than the

rate with which the NS can expel the material (using the Eddington accretion luminosity as powering mechanism), then a CE may form. Using the fact that the NS is the less massive component of the system, its Roche lobe in solar radii is $R_{\text{rl}} = 1.9 M_{\text{NS}}^{1/3} P_d^{2/3}$ (here P_d is the orbital period in days). The estimate for the critical mass transfer rate is then:

$$\dot{M}_{\text{crit}} \approx 2 \times 10^{-3} M_{\text{NS}}^{1/2} P_d^{2/3} M_{\odot} \text{ yr}^{-1}. \quad (15)$$

We estimate that systems with the maximum mass transfer rate of about $\dot{M}_{\text{trap}} \approx 10^{-3} M_{\odot} \text{ yr}^{-1}$ and orbital periods $P_d \leq 0.3^d$ will satisfy the condition that $\dot{M}_{\text{trap}} > \dot{M}_{\text{crit}}$ for CE formation.

Although our current understanding is not sufficiently developed to conclude with certainty that CE evolution will ensue if the above critical rate is exceeded, this remains a possibility. In this context, comparison of the calculated mass transfer rates of our sequences with \dot{M}_{crit} leads to the conclusion that the formation of a CE via this mechanism is, indeed, possible (see Figure 1). The duration of this unstable phase (when the mass transfer rate exceeds \dot{M}_{crit}) depends on the evolutionary stage of the helium star, and ranges from a few hundred years, if the critical mass transfer rate is achieved during He-shell burning (case B), to a few years, if the critical mass transfer rate is achieved after core-C ignition (case B or C). In the latter case the spiral-in timescale could be longer than the helium star evolutionary timescale. This is expected since, in this case, the mass in the stellar envelope is comparable to or less than the NS mass and significant spin-up of the common envelope is possible, prolonging the spiral-in phase (Sandquist et al. 2000). We therefore expect that for a CE phase developing in the very advanced evolutionary phases of the helium star the spiral-in will not be completed before the helium star ends its evolution in a supernova and a DNS forms.

The overall results of the most important evolutionary sequences are listed in Table 1. Specifically, the final orbital periods P_f , total mass $M_{\text{He};f}$ and envelope mass $M_{\text{env};f}$ of the evolved helium stars are presented. The mass of the helium envelope is given at the end of the first mass transfer stage as well as the final envelope mass at the end of the evolution. The mass of the helium envelope is defined as the mass above the radius where the helium abundance is less than 1%.

In addition, we also provide an estimate of the thermal mass transfer rate, \dot{M}_{TH} , (i.e., the maximum mass transfer rate for which the star can remain in thermal equilibrium), where $\dot{M}_{\text{TH}} = \frac{\Delta M_{\text{env}}}{t_{\text{TH}}}$ and $t_{\text{TH}} = 1.5 \times 10^7 \frac{M_{\text{He}}^2}{R_{\text{He}} L}$ yr. Here R_{He} and L are the radius and luminosity of the helium star in solar units. It can be seen from Table 1 that the average mass transfer rate (for Case B) is greater than \dot{M}_{TH} in sequences for which the mass transfer is initiated at an earlier stage. Here, the average mass transfer rate is given by the ratio of the mass

lost to the duration of the mass transfer phase. On the other hand, mass transfer initiated soon after the HeMS results in a rate close to \dot{M}_{TH} . In this case, as the mass transfer rises above \dot{M}_{TH} , a delayed dynamical instability develops.

Our calculations have shown that stars less massive than $3.5 M_{\odot}$ can evolve into a common envelope during the second mass transfer event. For these sequences, the two stages of mass transfer take place after core-C and core-O ignition with the typical orbital periods corresponding to about 0.2 d at the onset of the second mass transfer event. Since, in this case, a significant amount of mass has already been lost during the evolution (see Table 1), it is highly likely that, if a CE is formed, the binary will survive the spiral-in phase and form a DNS. This follows from the fact that the orbital energy is significantly greater (by more than a factor of 10) than the energy required to drive the remaining envelope matter to infinity. As a result, the orbital shrinkage associated with this CE phase is not expected to differ very much from that predicted by the stable mass transfer sequences.

A summary of our results based on the outcome of the mass transfer phase is illustrated in Figure 3. We have found four qualitatively different outcomes, which depend on the mass of the helium star and its evolutionary stage or orbital period at the onset of mass transfer. These outcomes can be described as:

- (i) a delayed dynamical instability develops, probably leading to a merger (stars in Figure 3);
- (ii) mass transfer proceeds stably, the mass transfer rate exceeds \dot{M}_{crit} during He-shell burning (hereafter CEB case), and probably leads to a merger (solid circles in Figure 3);
- (iii) mass transfer started during or after He-shell burning and proceeds stably, but the mass transfer rate remains below \dot{M}_{crit} and a DNS is formed (triangles in Figure 3);
- (iv) mass transfer started during He-shell burning or after the core-C ignition and proceeds stably, the mass transfer rate exceeds \dot{M}_{crit} after core-C ignition (hereafter CEC case), and a DNS is likely formed (open circles in Figure 3);

3.2. Population Synthesis Models

To examine the implication of our mass transfer results for DNS formation we have run a few indicative models. Based on our earlier experience with modeling double compact

object formation (Belczynski et al. 2002b), we have chosen to present results for one representative population synthesis model consisting of a population of 10^6 primordial massive binary systems. The initial conditions and binary-evolution parameters (other than He-star mass transfer episodes) are consistent with the model A from Belczynski et al. (2002b). We obtain results for 3 different sets of assumptions regarding the behavior of He stars:

1. Roche lobe filling He stars are treated as described in § 2.2.
2. He stars less massive than $5 M_{\odot}$ that have evolved away from the HeMS experience stable mass transfer with mass loss and orbital period contraction similar to that seen in most of our mass-transfer sequences (and in Dewi et al. 2002). In all other cases He stars are assumed to experience a merger. In the stable mass transfer episodes the donors are assumed to lose their entire He-rich envelopes. Since mass transfer rates are much higher than the Eddington limit, we assume that all of the transferred material is lost from the systems with the specific orbital angular momentum of the NS (consistent with our detailed mass transfer sequences). During the mass transfer phase helium stars are not nuclearily evolved (we refer to this as model *MT+CEB+CEC*).
3. similar to model 2, except that systems in the CEB region (see Figure 3) lead to mergers (we refer to this as model *MT+CEC*).

In the synthesis calculations one can identify among DNS progenitors those systems with NS and He-stars that fill their Roche lobes after core-He burning ($\sim 80\%$ of all DNS progenitors). The period and He-star mass distributions of this population are shown in Figures 4 and 5 respectively. It can be seen that the mass distribution is bi-modal with broad peaks near $2.8 M_{\odot}$ and $4 M_{\odot}$, whereas the period distribution is singly peaked at an orbital period of 0.1 d with a tail extending to periods of greater than 1 day. The minimum helium star mass for NS formation in our population synthesis models of binary evolution is $\sim 2.3 M_{\odot}$, and it agrees very well with earlier estimates. We note that the lower He star mass limit for NS formation in single star evolution is $\sim 2.2 M_{\odot}$ (see Habets 1986) and may extend to as high as $\sim 2.5 M_{\odot}$ ($2.9 M_{\odot}$) for case BB (BA) mass transfer in binary evolution (see Dewi et al. 2002).

In Figure 6 we show the population in terms of helium star masses $M_{\text{He;tr}}$ and orbital periods P_{tr} at the onset of mass transfer. The lines separating the various types of outcomes are also shown (see Figure 3). A comparison between Figures 3 and 6 reveals that a significant fraction ($\sim 47\%$) of the mass-transferring DNS progenitors can probably avoid a merger: (i) systems between solid lines (excluding dashed zones) never develop a dynamical instability nor do they exceed \dot{M}_{crit} (given in eq. 15), (ii) systems within the long-dashed line exceed

\dot{M}_{crit} late enough that we expect them to avoid a merger. We have also examined two other models for 2 different values of the $\alpha_{\text{CE}}\lambda$ parameter. The fraction of the mass-transferring DNS progenitors that can probably avoid a merger are $\sim 47\%$ (for $\alpha_{\text{CE}}\lambda = 0.3$) and $\sim 65\%$ (for $\alpha_{\text{CE}}\lambda = 3$).

In Figure 7 we present the derived distributions of DNS lifetimes (i.e., the time within which the two NS merge due to gravitational-wave radiation) under the 3 different assumptions described above. It is evident that the two more realistic models 2 and 3 lead to formation of DNS with longer lifetimes than model 1. However, the differences between the distributions do not have drastic implications. The stable mass transfer model 2 results in about one order of magnitude longer merger lifetimes of DNS. The distributions are not greatly dissimilar because the orbital contraction in the assumed CE evolution scenario 1 is not very dramatic due to the small masses of the He-star envelopes (ejection of the small envelope does not lead to drastic orbital contraction). In the stable mass transfer sequences (model 2) there is significant orbital contraction, because mass is transferred from the more massive to the less massive binary component. Consequently, short-lived DNS systems ~ 10 Myr (compared to 1-10Gyr previously expected) can still form as found in Belczynski et al. (2002b). In model 3 many more DNS progenitors merge and therefore the number of short-period DNS is depleted compared to the case with stable mass transfer. We find DNS Galactic merger rate in 3 models considered as follows: 53, 56 and 33 DNS mergers per Myr respectively for model 1, 2 and 3.

The merger time distributions of DNS systems for both alternative CE models with $\alpha_{\text{CE}}\lambda = 0.3$ and $\alpha_{\text{CE}}\lambda=3.0$ are very similar. Both distributions peak at around 10-100 Myrs with the majority of systems having merger times between $0.1 - 10^4$ Myrs. The distribution for $\alpha_{\text{CE}}\lambda = 0.3$ shows a slight overabundance of systems with very short merger times. This may be ascribed to the fact that all DNS progenitors have experienced CE, and in the model with small CE efficiency, they have formed tighter systems (and thus with shorter merger times) than for models with large CE efficiency. In general the two additional models resemble very closely the distribution obtained for our standard model with $\alpha_{\text{CE}}\lambda = 1.0$ shown with in Fig.7 (solid line). The lack of strong dependence of the merger time distribution on CE efficiency parameters reflects the fact that the last MT episode leading to the formation of DNS does not involve a CE. Therefore, by varying the values of CE parameters, we substantially alter the population of binaries entering the last MT episode. Nevertheless this final MT stage acts as a filter, allowing only systems with similar properties to eventually become coalescing DNS.

4. CONCLUSIONS

We have undertaken a comprehensive study of the DNS formation via the helium star - NS binary formation channel. We have calculated a suite of 60 evolutionary sequences, and delineated the mass $M_{\text{He;tr}}$ and orbital period P_{tr} regimes where systems evolve stably and where they undergo CE evolution. The numerical results reveal the classification of binary systems depending on the type of the mass transfer during their evolution and the outcome of this mass transfer phase. The classification can be described as:

1. Unstable mass transfer that leads to a delayed dynamical instability (DDI) and a binary merger, aborting DNS formation:
 - (a) Binaries with mass ratios (at the onset of the mass transfer) greater than 3.5
 - (b) Systems with HeMS donors (corresponding to orbital periods less than about 0.1d for $M_{\text{He}} < 5M_{\odot}$ and less than 0.5d for $M_{\text{He}} > 5M_{\odot}$)

2. Stable mass transfer (possibly in 2 phases interrupted by a detached phase):
 - (a) For Roche lobe overflow during the He-shell burning phase, the helium star component can lose nearly its entire envelope before the core-C ignition takes place (first contact phase). The mass transfer phase can be interrupted at the end of the He-shell burning stage when the binary usually becomes detached. If this detached stage precedes core-C ignition, a second mass transfer event ensues during and after core-C burning.
 - (b) CE phase may occur as a result of the accretion trapping radius exceeding the Roche lobe radius of the NS:
 - i. in systems with $P_{\text{tr}} \lesssim 0.3$ days for $M_{\text{He;tr}} < 5M_{\odot}$ the mass transfer rate exceeds \dot{M}_{crit} during the He-shell burning; these systems are likely to merge
 - ii. in systems with $P_{\text{tr}} \approx 0.1-0.5$ days for low He-star masses ($\sim 2.6-3.3 M_{\odot}$) the mass transfer rate exceeds \dot{M}_{crit} after core-C ignition; binaries survives and a DNS is likely formed.

In the case of stable mass transfer without the occurrence of the CE, typically, the amount of envelope mass that remains at the end of the evolution depends on the duration of the mass transfer: the earlier mass transfer occurs, the smaller the remaining envelope mass. Our results suggest that close systems consisting of low-mass helium stars ($\lesssim 3.5M_{\odot}$) lose a significant fraction of their envelopes (see Table 1), especially if they evolve through a second phase of mass transfer. Such systems are one of the possible types of binary progenitor

candidates for Type Ic supernovae (see also Dewi et al. 2002). However the contribution of this channel is only about 1% of the total Ic supernovae rate (0.7% if CE phase occurred during the He shell burning). As a result of the mass transfer, the systems evolving through stable mass transfer form a short period population of immediate DNS progenitors with periods ranging from 0.03 d to 1.7 d.

We have classified binary systems as possible mergers if CE occurred and the binding energy of the common envelope is greater than the energy released from the orbit. Such merged models leading to the formation of a black hole and a helium rich accretion disk have been discussed as potential progenitor candidates of γ -ray bursts (Fryer & Woosley 1998, Zhang & Fryer 2001). These mergers may increase previously predicted rates of γ -ray bursts (Fryer, Woosley & Hartman 1999; Belczynski et al. 2002c). The rate is about 0.5% of the total supernovae rate (all types), if one assumes that only mergers of He stars more massive than $4 M_{\odot}$ produce γ -ray bursts (0.7% if CE events occurred during the He shell burning). If one assumes that γ -ray bursts can be produced by NS merger with the He star more massive than $2.3 M_{\odot}$, the corresponding rates are 1.7% and 2.2% of the total supernova rate.

We note that the CE phase could be avoided if the critical mass transfer rate occurs after the core-O ignition when the nuclear evolutionary timescale becomes shorter than the spiral-in timescale.

The short orbital periods of the immediate progenitor systems of DNS have important implications for the distribution of DNS merger times. In comparison to Belczynski et al. (2002b), it is found that the fraction of very short-lived (< 1 Myr) DNS systems decreases since the majority of DNS progenitors evolve through a stable mass transfer phase rather than through a CE phase with the survival. Although the peak of the distribution occurs at merger times $\sim 2 - 12$ Myr, very short-lived systems are still formed at significant rates since orbital contraction is non-negligible for the stable mass transferring systems. In particular, for the models that we examined, the fraction of short-lived (< 1 Myr) DNS binaries is reduced from $\simeq 50\%$ (27 mergers per Myr in our Galaxy) to $\simeq 15\%$ (8 mergers per Myr in our Galaxy). As pointed out by Belczynski & Kalogera (2001) and discussed also by Belczynski et al. (2002b), a population of such short-lived DNS has implications for the estimates of coalescence rates based on the currently observed DNS sample, which consists only of long-lived systems ($\gg 1$ Myr). In view of our results in this study, the associated upward correction factors for such empirical rate estimates are modified and are $\simeq 1.3$ (instead of 2.5 as estimated by Belczynski et al. (2002b)). However, in the case where CE phase occurs during He shell burning, the number of short-period binaries vanishes.

The lifetimes of DNS systems also have important implications for the typical galactocentric distances of DNS merger sites and their possible association with γ -ray bursts (Bloom, Kulkarni, & Djorgowski 2002). In view of this reduced fraction of very short-lived DNS, we have re-examined the cumulative distributions of the projected galactocentric distances of DNS merger sites [for details see Belczynski et al. (2002a)]. In Figure 8 we present the distributions for the 3 cases considered in §3.2. The initial distribution of primordial binaries in a galaxy is also shown for comparison. The farther a given model deviates from the initial distribution, the farther is the location of merger sites from the center of the galaxy. Calculations for galaxies similar in size and mass to the Milky Way, and for dwarf galaxies with 1% of the Milky Way mass have been performed [for details see Belczynski et al. (2002c)].

It is evident that, in the case of large galaxies like the Milky Way, there is little difference compared to the results of Belczynski et al. (2002a) and the DNS mergers, whichever model is used, take place inside the larger, massive hosts. Even for moderately long-lived systems, the deep gravitational potential of massive galaxies as well as its large size prevents DNS from escaping far from the galaxy borders before their coalescence due to gravitational wave radiation. Therefore, even for two different populations of DNS (with very short merger times for CE evolutionary model and short merger times for stable mass transfer model) their merger locations are basically indistinguishable.

For the smallest and lowest mass galaxies, there are noticeable differences between the distributions. Since low-mass galaxies have a very small effect on fast moving DNS, even small differences in merger times are imprinted on the location of merger sites. The longer the merger time the farther the system will escape from the host galaxy. For the model in which the immediate DNS progenitor survive CE evolution, model 1, only a small fraction ($\sim 10\%$) of DNS will merge outside the low mass hosts. On the other hand, for models representing our new calculations we find that up to 20% of DNS mergers may take place outside such galaxies (30% in model 2). Nevertheless, this is in stark contrast to the previous population synthesis results, predicting that as many as $\sim 50 - 80\%$ of DNS should escape their host galaxies (e.g., Bloom et al. 1999; Portegies Zwart et al. 1999; Bulik et al. 1999). Therefore, assuming that some γ -ray bursts are connected to DNS mergers, it is most likely that they occur within their galaxies.

We would like to thank C. Fryer, N. Langer, O. Pols, and R.F. Webbink for useful discussions. This work is partially supported by the Lindheimer Fund at Northwestern University, and NSF grant PHY-0121420 to VK, NSF grant PHY-0133425 to FR, and AST-9727875 and AST-0200876 to RT. VK also acknowledges support by the David and Lucide Packard Foundation through a Science and Engineering Fellowship.

REFERENCES

- Alexander, D. R., & Ferguson, J. W. 1994, *ApJ*, 437, 879
- Angulo, C., et al. 1999, *Nucl. Phys.*, A656, 3
- Begelman, M. 1979, *MNRAS*, 197, 237
- Belczynski, K., Bulik, T., & Kalogera, V. 2002a, *ApJ*, 571, L147
- Belczynski, K. & Kalogera, V. 2001, *ApJ*, 550, L183
- Belczynski, K., Kalogera, V., & Bulik, T. 2002b, *ApJ*, 572, 407
- Belczynski, K., Bulik, T., Rudak, B. 2002c, *ApJ*, 571, 394
- Bethe, H., & Brown, G. E. 1998, *ApJ*, 506, 780
- Bhattacharya, D., & van den Heuvel, E.P.J. 1991, *Phys. Rep.*, 203, 1
- Bloom, J.S., Sigurdsson, S., & Pols, O.R. 1999, *MNRAS*, 305, 763
- Bloom, J.S., Kulkarni, S.R., & Djorgowski, S.G. 2002, *AJ*, 123, 1111
- Brown, G.E. 1995, *ApJ*, 440, 270
- Bulik, T., Belczynski, K., & Zbijewski, W. 1999, *MNRAS*, 309, 629
- Cannon, R.C. 1993, *MNRAS*, 263, 817
- Clark, J. P. A., & Eardley, D. M. 1977, *ApJ*, 215, 311
- Cordes, J.M., & Chernoff, D.F. 1998, *ApJ*, 505, 315
- Dewi, J. D. M. & Tauris, T. M. 2000, *A&A*, 360, 1043
- Dewi, J. D. M., Pols, O. R., Savonije, G. J., van den Heuvel, E. P. J. 2002, *MNRAS*, 331, 1027
- Eggleton, P. P. 1983, *ApJ*, 268, 368
- Fryer, C.L., 1999, *ApJ*, 522, 413
- Fryer, C.L., Woosley, S.E. 1998, *ApJ*, 502, L9
- Fryer, C.L., Woosley, S.E., & Hartmann, D.H. 1999, *ApJ*, 526, 152

- Habets, G. M. H. J. 1986, *A&A*, 167, 61
- van den Heuvel, E. P. J. 1994, *A&A*, 291, L39
- van den Heuvel, E. P. J., & Taam, R. E. 1984, *Nature*, 309, 235
- Hjellming, M.S. 1989, Ph.D. thesis, University of Illinois
- Hurley, J. R., Pols, O. R., Tout, C. A. 2000, *MNRAS*, 315, 543
- Hut, P. 1980, *A&A*, 92, 167
- Kalogera, V., Webbink, R. F. 1996, *ApJ*, 458,301
- King, A.R., & Begelman, M. 1999, *ApJ*, 519, L169
- Kippenhahn, R., Weigert, A., & Hofmeister, E. 1967, in *Methods in Computational Physics*, Vol. 7, ed. B. Alder, S. Fernbach, & M. Rothenberg (New York: Academic), 129
- de Kool, M. 1990, *ApJ*, 358, 189
- Landau, L.D.,& Lifshitz, E.M. 1958, *The classical theory of fields*, Pergamont Press, Oxford
- Nomoto, K., Yamaoka, H., Pols, O. R., van den Heuvel, E. P. J., Iwamoto, K., Kumagai, W., Shigeyama, T. 1994, *Nature*, 371, 227
- Paczynski, B. 1986, *ApJ*, 308, L43
- Perna, R., & Belczynski, K. 2002, *ApJ*, 570, 252
- Podsiadlowski, Ph., Rappaport, S., & Pfahl, E. 2002, *ApJ*, 565, 1107
- Pols, O.R., 2002, private communication
- Portegies Zwart, S.F., & Yungelson, L.R. 1998, *A&A*, 332, 173
- Rasio, F. 1996, in *Evolutionary Processes in Binary Stars*, ed. R. A. M. J. Wijers, M. B. Davies, & C. A. Tout (Dordrecht: Kluwer), 121
- Ritter, H. 1988, *A&A*, 202, 93
- Rogers, F. J., & Iglesias, C. A. 1992, *ApJS*, 79, 507
- Sandquist, E.L., Taam R.E., & Burkert, A. 2000, *ApJ*, 533, 984
- Soberman, G. E., Phinney, E. S., van den Heuvel, E. P. J. 1997, *A&A*, 327, 620

- Taam, R. E., & Sandquist, E. 2000, *ARAA*, 38, 113
- Thielemann, F.-K., Truran, J. W., & Arnould, M., in *Advances in nuclear astrophysics*, ed. Frontieres (Gif-sur-Yvette, France), 1986, p. 525
- Tout, C. A., Eggleton, P. P. 1988, *ApJ*, 334, 357
- Tutukov, A.V & Yungelson, L. 1979, in “Mass Loss and Evolution of O-type stars”, Symposium No. 83, eds. P. Conti & C.W.H. de Loore (Dordrecht: Reidel), p. 151
- Webbink, R. 1985, in *Interacting Binary Stars*, ed. J.E. Pringle & R.A. Wade (Cambridge:Cambridge University Press), 39
- Woosley, S.E. 1986, in “Nucleosynthesis and Chemical Evolution”, 16th Saas-Fee Course, eds. B.Hauck et al., Geneva Obs., p.1
- Woosley, S.E. 1997, private communication
- Woosley, S.E., Langer, N., & Weaver, T.A. 1995, *ApJ*, 411, 823
- Zhang, W., & Fryer, C.L. 2001, *ApJ*, 550, 357

Table 1. The binary parameters and outcomes of representative model sequences. The columns denote: the mass, $M_{\text{He};0}$ (in M_{\odot}) on the zero age helium main sequence, the mass, $M_{\text{He};\text{tr}}$ (in M_{\odot}), the mass of the envelope, $M_{\text{env};\text{tr}}$ (in M_{\odot}), orbital separation, A_{tr} (in R_{\odot}), orbital period P_{tr} (in days), at the onset of mass transfer; \dot{M}_{TH} (in $M_{\odot}\text{yr}^{-1}$) is the thermal timescale mass transfer rate. The evolutionary stages are denoted as case A for Roche lobe overflow on HeMS, case B during He-shell burning, and case C for phases after carbon ignition. The possible outcomes are: DDI for delayed dynamical instability (that leads to a merger), CEB for possible CE formation during He-shell burning (likely to lead to a merger), CEC for possible CE formation after core-C ignition (DNS is likely formed), MT when CE did not occur (DNS is formed), and NC denoted the boundary case when the system did not interact (for all periods larger than cited in the table, mass transfer will not occur). For models that do not experience DDI, but interact, we list the final period, P_{f} (in days), the final mass of the helium star, $M_{\text{He};\text{f}}$ (in M_{\odot}), the final mass of the envelope, $M_{\text{env};\text{f}}$ (in M_{\odot}), and the duration of the mass transfer episode, Δt_{tr} in years. The duration of mass transfer is calculated from the onset of Roche lobe overflow to the ignition of oxygen in the core (end of model calculations) or to the detachment of the He star from its Roche lobe (MT cases), whichever occurs earlier. If only one mass transfer phase was encountered, there is one entry in the Δt_{tr} column. A second entry indicates that the mass transfer stopped but was then reinitiated and the duration of the second mass transfer phase is given. The first entry in the $M_{\text{env};\text{f}}$ column always represents its value at the end of the first mass transfer phase. The second entry, if present, indicates that the first mass transfer phase finished before the end of our evolutionary calculations (core-O ignition). We list the envelope mass at the end of the model calculations, depleted (in relation to the first entry) either through the second mass transfer event or by wind mass loss.

$M_{\text{He};0}$	$M_{\text{He};\text{tr}}$	$M_{\text{env};\text{tr}}$	A_{tr}	P_{tr}	\dot{M}_{TH}	Case	outcome	P_{f}	$M_{\text{He};\text{f}}$	$M_{\text{env};\text{f}}$	Δt_{tr}
6.0	4.99	1.91	0.99	0.045	$1.7 \cdot 10^{-4}$	B	DDI	–	–	–	–
6.0	4.97	1.88	1.68	0.1	$4.0 \cdot 10^{-4}$	B	DDI	–	–	–	–
6.0	4.96	1.85	2.66	0.2	$6.8 \cdot 10^{-4}$	B	DDI	–	–	–	–
6.0	4.95	1.80	3.43	0.3	$9.2 \cdot 10^{-4}$	C	CEC	0.23	3.94	0.69	$2.3 \cdot 10^3$
6.0	4.95	1.78	4.15	0.4	$1.1 \cdot 10^{-3}$	C	DDI	–	–	–	–
6.0	4.95	1.68	5.0	0.52	–	–	NC	–	–	–	–
5.0	4.32	1.99	1.45	0.085	$3.2 \cdot 10^{-4}$	B	DDI	–	–	–	–
5.0	4.32	1.82	1.6	0.1	$3.2 \cdot 10^{-4}$	B	CEB	0.027	2.88	0.57/0.3	$3.3 \cdot 10^3/34$
5.0	4.32	1.80	3.35	0.3	$8.2 \cdot 10^{-4}$	B	CEB	0.088	3.01	0.73/0.42	$5.1 \cdot 10^3$
5.0	4.31	1.76	4.00	0.39	$1.0 \cdot 10^{-3}$	C	MT	0.14	3.24	0.58	$5.5 \cdot 10^3$
5.0	4.29	1.67	9.2	1.4	–	–	NC	–	–	–	–
4.0	3.62	–	1.3	0.075	–	A	DDI	–	–	–	–
4.0	3.58	1.60	1.46	0.1	$2.5 \cdot 10^{-4}$	B	CEB	0.041	2.34	0.73/0.3	$4.8 \cdot 10^3/1 \cdot 10^4$
4.0	3.54	1.53	2.31	0.2	$4.6 \cdot 10^{-4}$	B	CEB	0.089	2.49	0.49/0.38	$1.1 \cdot 10^4$
4.0	3.51	1.50	3.05	0.3	$6.4 \cdot 10^{-4}$	B	MT	0.14	2.52	0.58/0.38	$7.8 \cdot 10^3/1.3 \cdot 10^3$
4.0	3.50	1.46	3.76	0.4	$8.2 \cdot 10^{-4}$	B	MT	0.21	2.62	0.60/0.45	$6.5 \cdot 10^3/1.3 \cdot 10^3$
4.0	3.50	1.46	4.96	0.6	$1.1 \cdot 10^{-3}$	C	MT	0.16	3.46	0.51	$1.1 \cdot 10^4$
4.0	3.50	1.46	7.0	1.0	$1.5 \cdot 10^{-3}$	C	MT	0.98	3.47	1.42	520
4.0	3.50	1.46	17.0	3.7	–	–	NC	–	–	–	–

Table 1—Continued

$M_{\text{He};0}$	$M_{\text{He};\text{tr}}$	$M_{\text{env};\text{tr}}$	A_{tr}	P_{tr}	\dot{M}_{TH}	Case	outcome	P_{f}	$M_{\text{He};\text{f}}$	$M_{\text{env};\text{f}}$	Δt_{tr}
3.5	3.22	–	1.07	0.06	–	A	DDI	–	–	–	–
3.5	3.21	1.55	1.49	0.1	$2.2 \cdot 10^{-4}$	B	MT	0.055	1.94	1.08/0.12	$7.8 \cdot 10^3 / 2.4 \cdot 10^4$
3.5	3.19	1.49	2.37	0.2	$4.4 \cdot 10^{-4}$	B	MT	0.12	2.11	0.47/0.14	$1.9 \cdot 10^4 / 2.9 \cdot 10^3$
3.5	3.19	1.48	3.12	0.3	$5.1 \cdot 10^{-4}$	C	CEC	0.17	2.08	0.50/0.21	$1.2 \cdot 10^4 / 8.1 \cdot 10^3$
3.5	3.19	1.48	3.75	0.4	$7.6 \cdot 10^{-4}$	C	CEC	0.23	2.13	0.54/0.25	$8.3 \cdot 10^4 / 7.8 \cdot 10^3$
3.5	3.19	1.48	4.84	0.6	$1.0 \cdot 10^{-3}$	C	MT	0.23	2.177	0.32	$1.9 \cdot 10^4$
3.5	3.16	1.27	27.8	8	–	–	NC	–	–	–	–
3.0	2.91	–	1.06	0.06	–	A	DDI	–	–	–	–
3.0	2.80	1.39	1.50	0.1	$1.9 \cdot 10^{-4}$	B	CEC	0.08	1.69	0.30/0.10	$5.7 \cdot 10^4 / 770$
3.0	2.78	1.37	2.37	0.21	$3.8 \cdot 10^{-4}$	B	CEC	0.16	1.76	0.38/0.11	$2.8 \cdot 10^4 / 2.5 \cdot 10^3$
3.0	2.78	1.36	2.98	0.3	$5.3 \cdot 10^{-4}$	B	MT	0.22	1.86	0.42/0.22	$1.8 \cdot 10^4 / 5.6 \cdot 10^3$
3.0	2.77	1.32	3.66	0.4	$6.4 \cdot 10^{-4}$	B	MT	0.3	1.81	0.46/0.16	$1.3 \cdot 10^4 / 1.1 \cdot 10^4$
3.0	2.77	1.22	10.6	2.0	$2.0 \cdot 10^{-3}$	C	MT	1.7	2.54	0.96	$2.6 \cdot 10^3$
3.0	2.76	1.14	35.8	25.0	–	–	NC	–	–	–	–

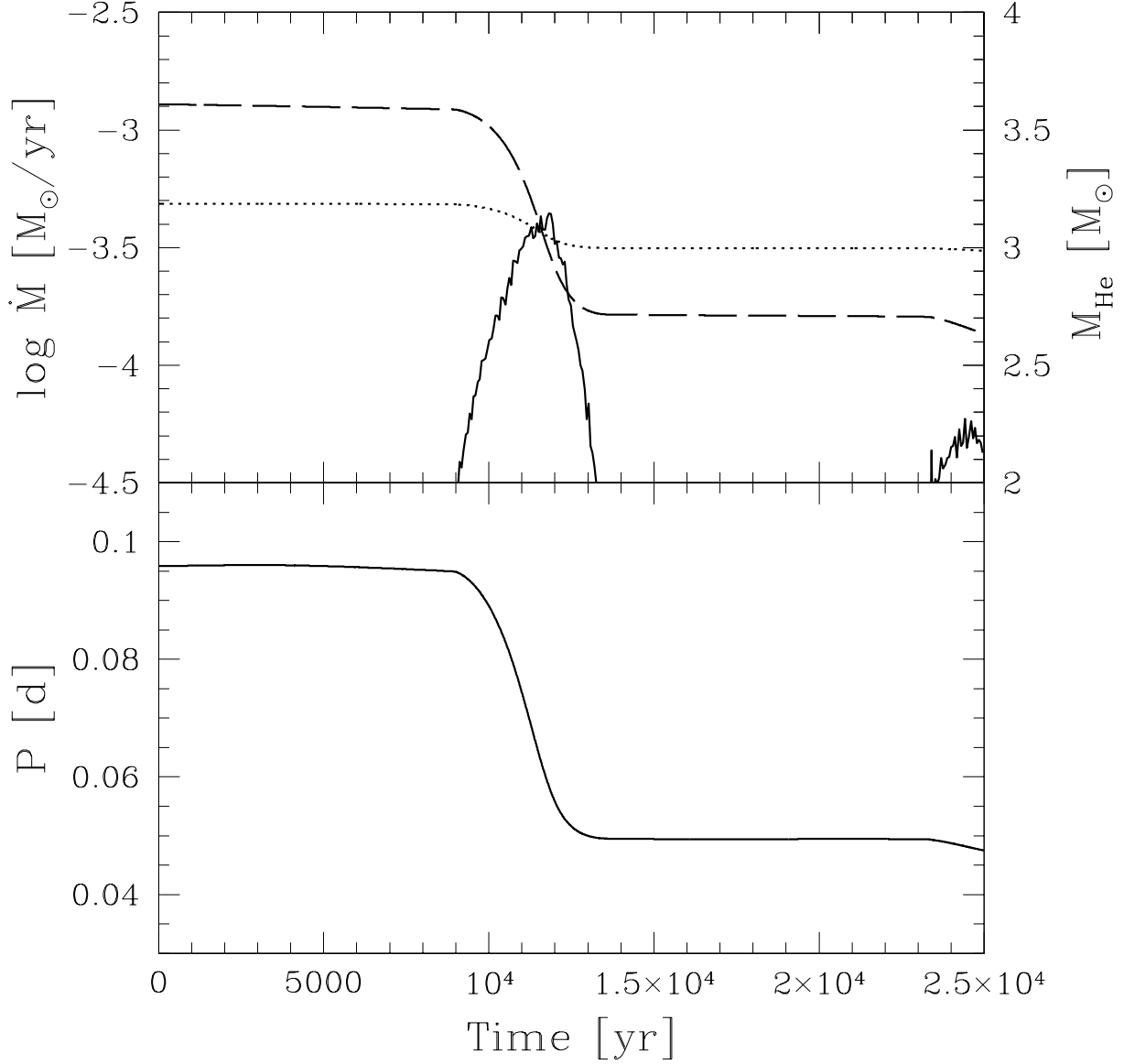


Fig. 1.— Evolution of a $4M_{\odot}$ He-star (mass at the zero age helium main sequence) and $1.4M_{\odot}$ NS binary with an orbital period at the onset of mass transfer of 0.096 d. Mass transfer begins during He-shell burning for the He-star donor. The time evolution of the mass transfer rate and the He-star mass are shown in the upper panel (solid and dashed lines, respectively) and the binary orbital period evolution is presented in the lower panel. The critical mass transfer rate (eq.15) for possible onset of a CE phase is also shown in the upper panel (dotted line). Note also the second mass transfer phase initiated after core-C ignition (lower right corner in the upper panel). The zero of time corresponds to the start of the mass transfer sequence when the age of the primary is $1.4 \cdot 10^6$ years

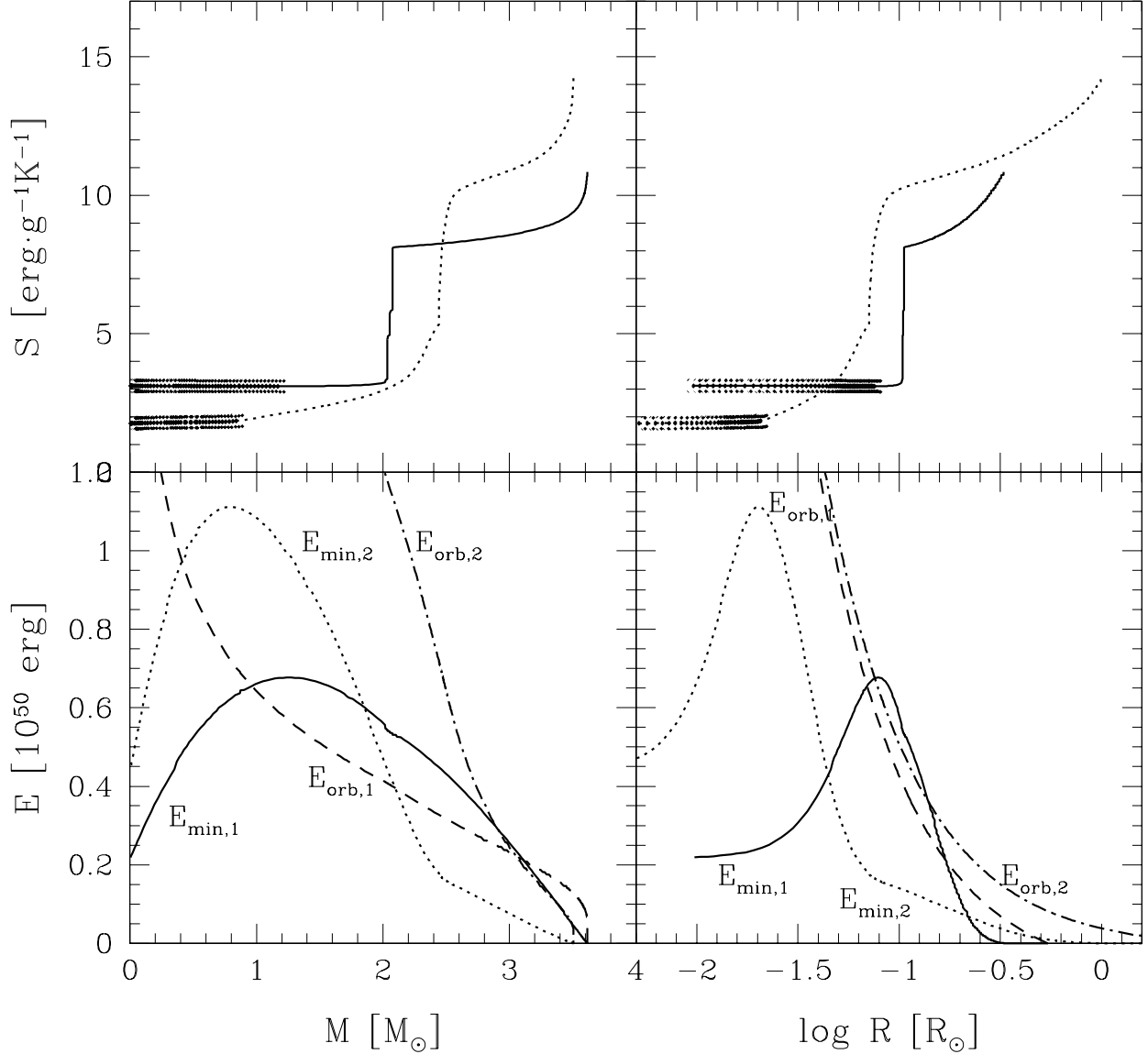


Fig. 2.— Specific entropy (upper panels) and energies (lower panels) as functions of mass (left panels) and radius (right panels) for a $4 M_\odot$ He-star at two different evolutionary stages: soon after the HeMS (solid lines in upper panels, index 1 in lower panels) and during core-C burning (dotted lines in upper panels, index 2 in lower panels). Hatched regions show convective zones; note that convection develops only in the He-star core. Note also that the CE survival is likely only for the evolved He-star (core-C burning), since the orbital energy (E_{orb}) is significantly greater than the energy needed to unbind its envelope (E_{min}). Orbital energies were calculated for a Roche-lobe filling $4 M_\odot$ He-star (initial mass) in orbit around a $1.4 M_\odot$ NS. The corresponding orbital periods are 0.075 and 1.2 days for models 1 and 2, respectively.

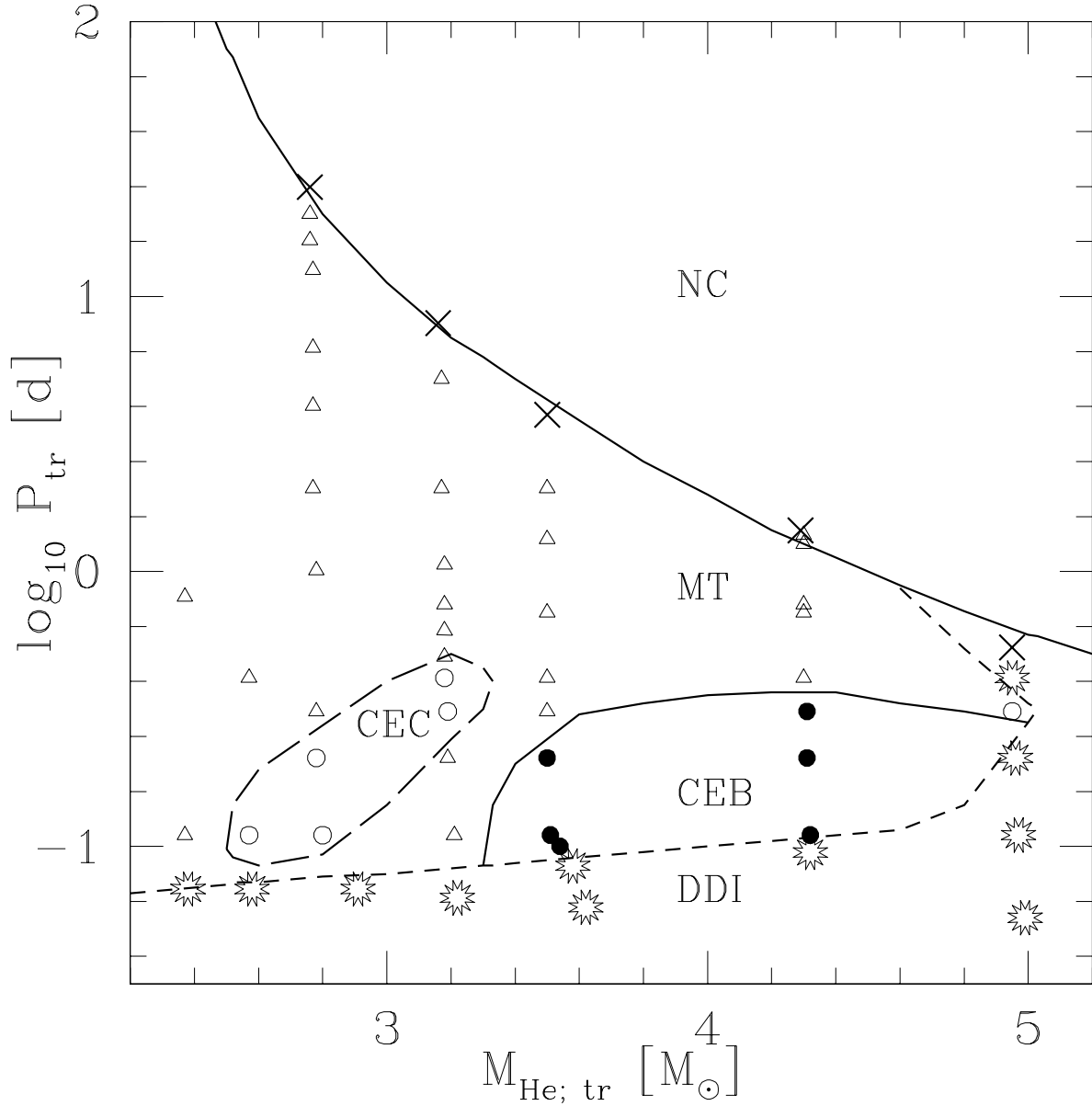


Fig. 3.— He-star masses $M_{\text{He;tr}}$ and orbital periods P_{tr} at the onset of mass transfer. Different symbols correspond to different outcomes of the mass transfer sequences: *crosses* – mass transfer never initiated; *triangles* – mass transfer rate never exceeds \dot{M}_{crit} and a DNS is formed; *open circles* – mass transfer rate exceeds \dot{M}_{crit} after core-C ignition (case C) and a DNS is likely formed; *filled circles* – mass transfer rate exceeds \dot{M}_{crit} during He-shell burning (case B) and the binary system will likely merge; *stars* – mass transfer leads to delayed dynamical instability and the binary system will likely merge. Lines delineate the boundaries between different outcomes in the $M_{\text{He;tr}} - P_{\text{tr}}$ parameter space.

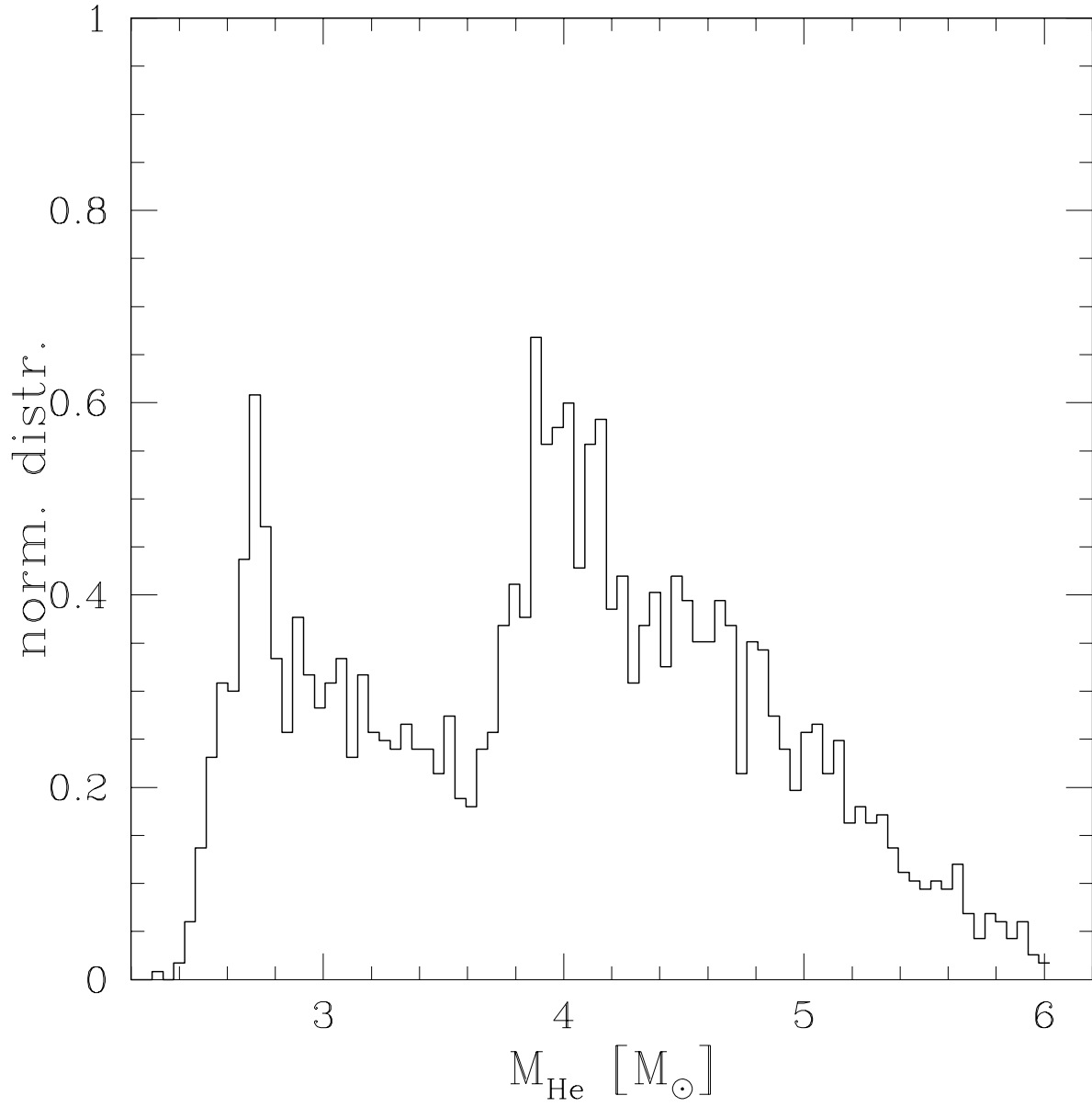


Fig. 4.— Normalized distribution of He-star masses at the onset of the mass transfer episode in potential DNS progenitors.

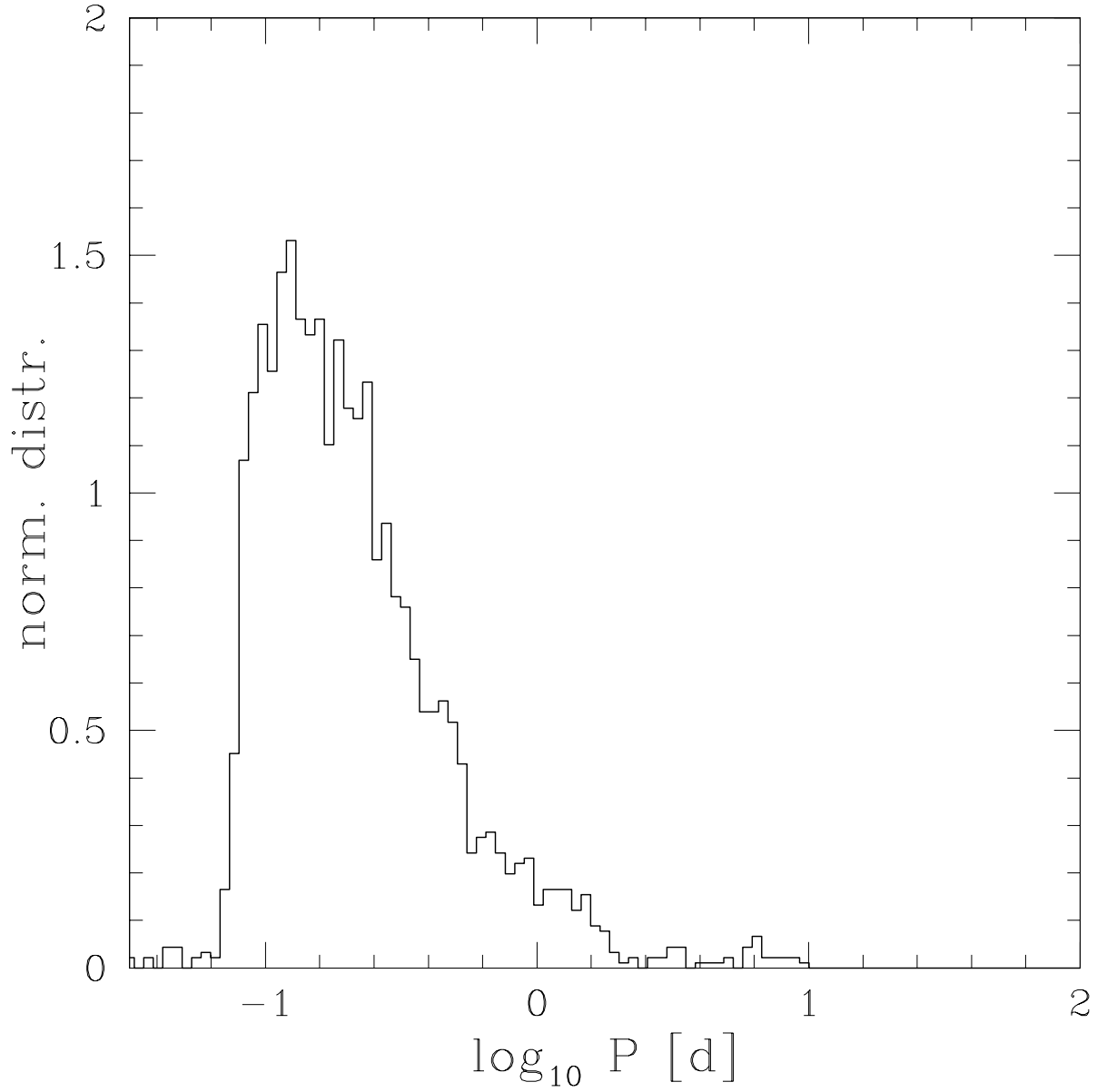


Fig. 5.— Normalized distribution of of orbital periods of potential DNS progenitors at the onset of the mass transfer episode.

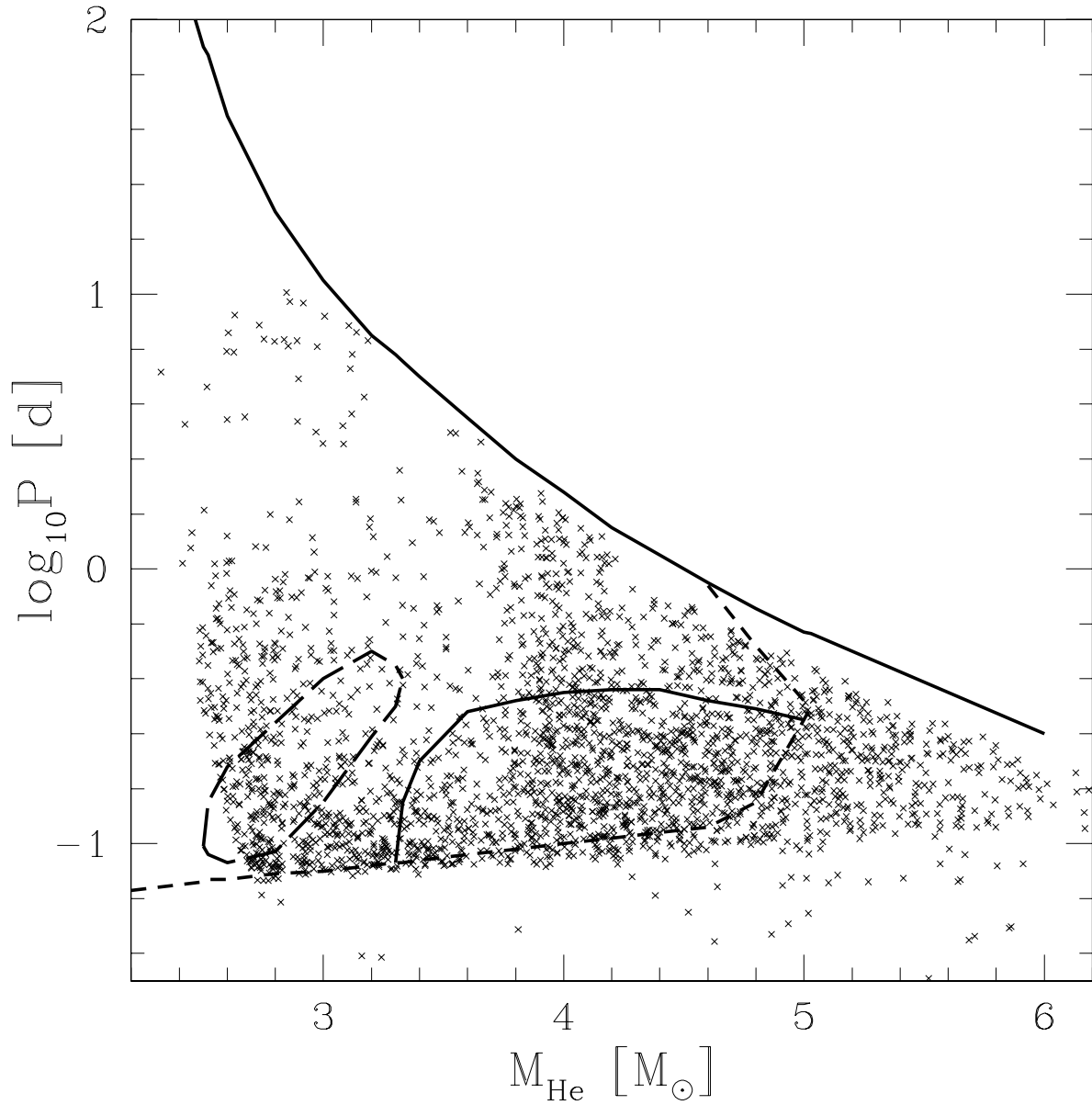


Fig. 6.— He-star masses and orbital periods of potential DNS progenitors that reach Roche lobe overflow after the end of core-He burning (HeMS), at the onset of the mass transfer episode. Lines correspond to the boundaries in Figure 3.

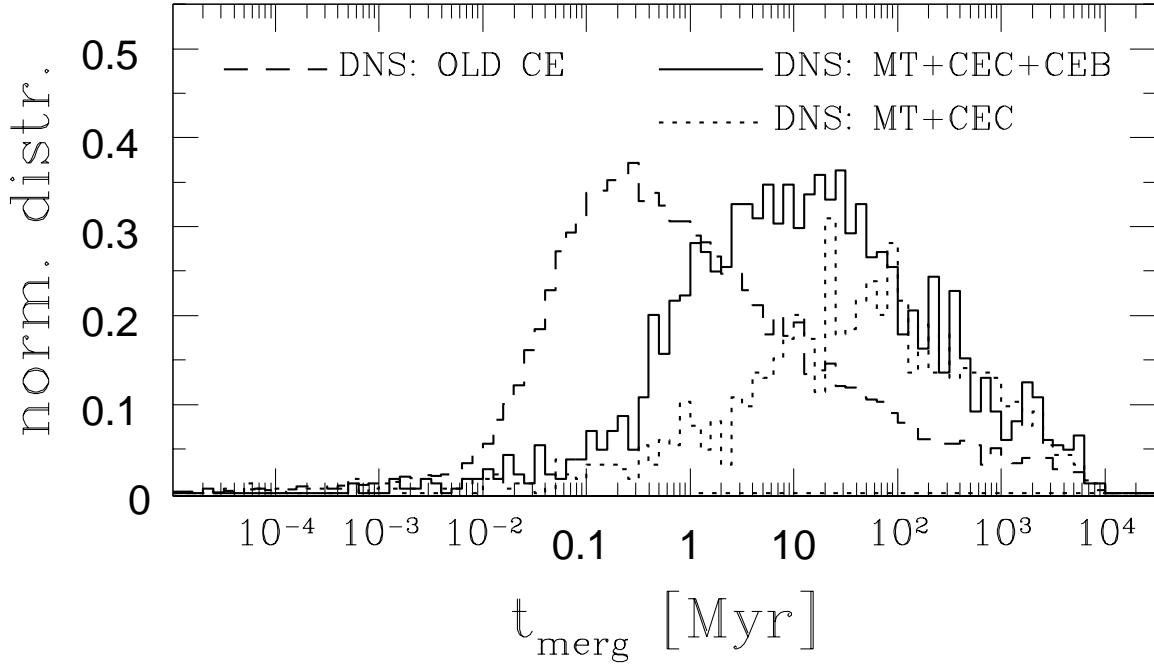


Fig. 7.— Normalized distribution of DNS merger lifetimes (due to gravitational radiation) under three different sets of assumptions about the outcome of mass transfer for He stars in binaries (from Figure 4): (i) systems with evolved He-star donors with $M_{\text{He}} \leq 4.5M_{\odot}$ go through CE evolution (as assumed in Belczynski et al. 2002b; dashed line), (ii) systems in the regions marked as MT, CEC and CEB in Figure 3 go through stable (but highly non-conservative) mass transfer (solid line), (iii) systems in the regions marked as MT and CEC go through stable mass transfer (dotted line), whereas systems from the region marked as CEB are assumed to merge.

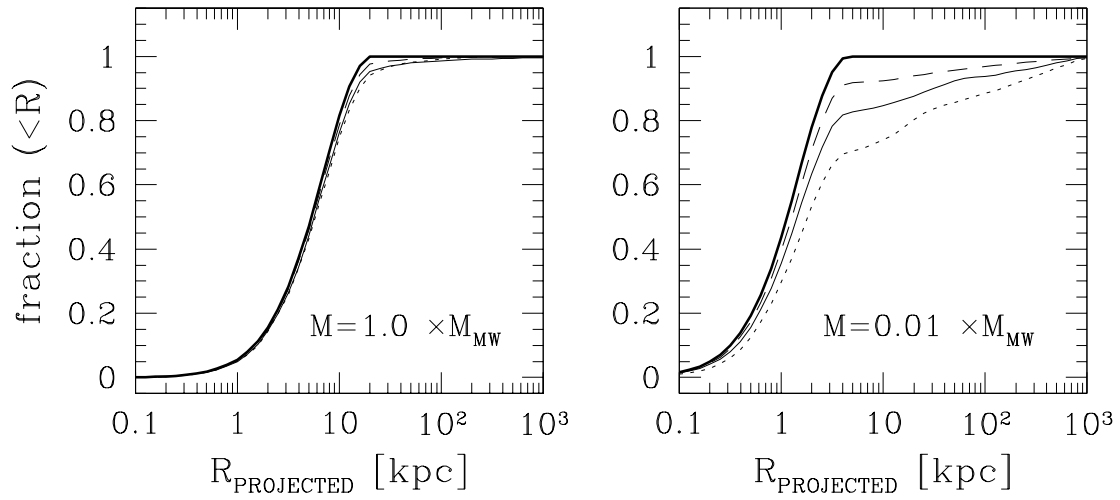


Fig. 8.— Cumulative distributions of DNS merger sites around a massive galaxy with $M = M_{\text{MW}} = 1.5 \cdot 10^{11} M_{\odot}$ (left panel) and a dwarf galaxy with $M = 0.001 \times M_{\text{MW}}$ (right panel). Thick solid lines correspond to the initial galactic distribution of binaries. Dashed lines correspond to DNS formed through CE evolution (assumed in Belczynski et al. 2002b), while thin solid and dotted lines correspond to DNS formed through stable mass transfer from the MT, CEC, and CEB groups or from only from the MT and CEC groups as marked in Figure 3, respectively.